

From Chromium–Chromium Quintuple Bonds to Molecular Squares and Porous Coordination Polymers

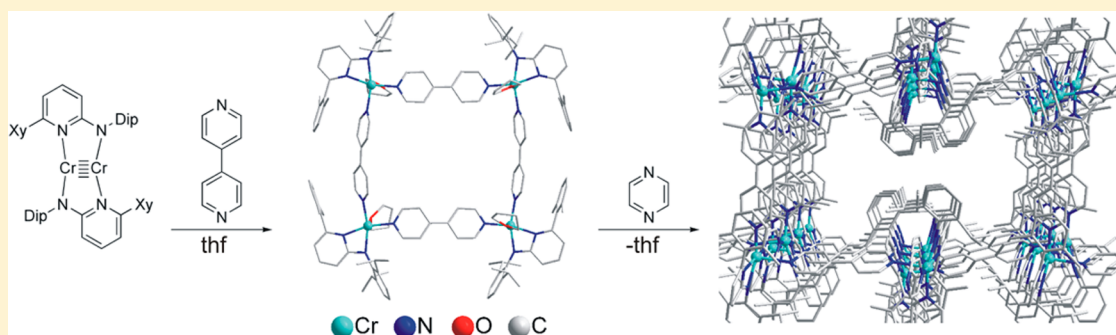
Awal Noor,[†] Emmanuel Sobgwi Tamne,[†] Benjamin Oelkers,^{†,||} Tobias Bauer,[†] Serhiy Demeshko,[‡] Franc Meyer,[‡] Frank W. Heinemann,[§] and Rhett Kempe^{*,†}

[†]Lehrstuhl Anorganische Chemie II, Universität Bayreuth, 95440 Bayreuth, Germany

[‡]Institut für Anorganische Chemie, Georg-August-Universität Göttingen, Tammannstraße 4, 37077 Göttingen, Germany

[§]Lehrstühle für Anorganische Chemie, Friedrich-Alexander-Universität Erlangen-Nürnberg, Egerlandstraße 1, 91058 Erlangen, Germany

S Supporting Information



ABSTRACT: Reaction of the quintuply bonded chromium(I) dimer [ApCrCrAp] (Ap = sterically demanding 2-aminopyridinate) with pyrazine yields a chromium(II) complex with a $\eta^4:\eta^4$ face-on coordinated pyrazine dianion. Reaction with 4,4'-bipyridine, on the other hand, completely cleaves the metal–metal bond, leading to a chromium(II)-based molecular square. XRD and magnetic measurements show ligand radical anions and a ferrimagnetic alignment of alternating metal and ligand magnetic moments. Controlled polymerization of the molecular square with pyrazine yields a porous coordination polymer featuring both reduced and nonreduced linkers.

INTRODUCTION

High bond orders have been a fascinating topic to scientists in general and chemists in particular for a long time.¹ Stable compounds featuring formal quintuple bonds were first presented in 2005 when Power and co-workers reported on the synthesis and structure of Ar'CrCrAr' (Ar' = 2,6-Dip-C₆H₃, Dip = 2,6-diisopropylphenyl).² Since then, chromium–chromium³ and molybdenum–molybdenum quintuple bonds⁴ are being intensively studied in order to integrate them into existing chemical bonding concepts. Very recently, an example of a heterobimetallic CrMn complex with a quintuple bond has also been reported.⁵ In the hunt for compounds with metal–metal distances as short as possible, diazalligands of the amidinate-, aminopyridinate- (Ap), and guanidinate-type proved to be particularly useful.⁶ In addition to theoretical investigations⁷ reactivity studies were utilized to gain insight into the properties of this new class of compounds.^{7–11}

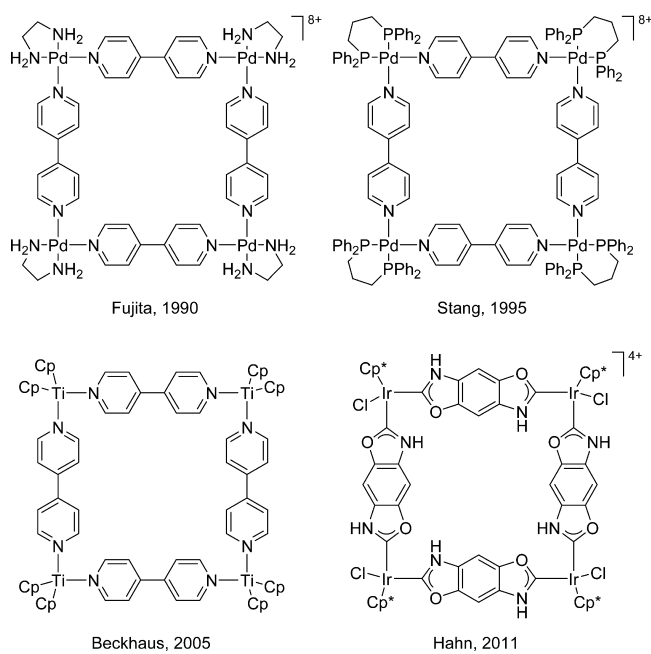
A rather different topic of contemporary coordination chemistry is concerned with self-assembled macrocyclic oligonuclear complexes, the most important of which are known as molecular squares.¹² Selected examples are shown in Scheme 1. Usually two *cis*-configured thermally or photochemically labile ligands are employed for generating the

necessary free coordination sites while the remaining ligand sphere is chosen to be sufficiently unreactive under the respective reaction conditions. The macrocycle is subsequently formed under thermodynamic control. Notably, different cyclic or polymeric species can be found in equilibrium with the tetranuclear complex. Another strategy was presented by Hahn and co-workers during studies on biscarbene linkers^{16,17} in that it is also possible to prepare the molecular square in two steps by using two different linkers or by modifying ligands within the metal's coordination sphere. The generation of coordinatively unsaturated, metal-centered building blocks can also be achieved by redox reactions of early transition metals in low oxidation states. Starting from a synthetic equivalent of titanocene, [Cp₂Ti{ η^2 -C₂(SiMe₃)₂}], Beckhaus and co-workers were able to obtain molecular squares with the classical linkers pyrazine and 4,4'-bipyridine (4,4'-bipy).^{15,18} In contrast to the majority of macrocycles featuring these bridging ligands, the N-heterocycles were found to be in reduced states in these complexes. As molecular squares are (at least in some instances) readily soluble compounds that still show a latent

Received: June 13, 2014

Published: November 10, 2014

Scheme 1. Selected Examples for Molecular Squares (Cp = C₅H₅; Cp* = C₅Me₅)^{13–16}



reactivity, they are candidates for the tailored generation of larger aggregates. Thus, a polymerization of molecular squares was recently demonstrated by Otsubo, Kitagawa, and co-workers by reacting a Pt-based square with iodine.¹⁹

As quintuply bonded chromium(I) dimers are coordinatively unsaturated, it seemed promising to react them with classical diaza linkers like pyrazine or 4,4'-bipyridine. Up to a certain N–N distance it should be possible to activate ligands at the diatomic platform without completely disrupting the Cr–Cr multiple bond. In the case of 4,4'-bipyridine, however, the (hopefully selective) formation of linkages between the metal centers seemed more likely. We report here on reactions of aminopyridinato ligand stabilized Cr–Cr quintuple bonds with pyrazine and 4,4'-bipyridine of which the latter leads to readily soluble molecular squares. These can be interconnected in a subsequent polymerization reaction, yielding porous coordination polymers (PCPs) in a controlled fashion.

RESULTS AND DISCUSSION

The reaction of the Ap-stabilized chromium complex **1** (a compound published by us already)⁹ with pyrazine in THF/hexane does not lead to a disruption of the metal–metal bond but to the green addition product **2** featuring *face-on* coordination of the heterocycle (Scheme 2, top). The X-ray diffraction study (XRD) shows that the aminopyridinate ligands are bent downward in comparison with **1**; their dihedral angle (N–Cr–N) amounts to about 102° (Figure 1). This gives rise to an empty upper hemisphere which is occupied by the pyrazine ligand in $\eta^4:\eta^4$ -coordination mode. The Cr–N bond lengths toward the Ap ligands lie between 204 and 207 pm and are thus in good agreement with the structurally related addition products of **1** with P₄,¹⁰ alkynes, and dienes.^{8a} The metal–metal distance amounts to about 192 pm which is significantly larger than in the starting material (175 pm⁹) as well as in the above-mentioned cycloadducts (180–190 pm^{8a,10}). The planarity of the pyrazine ring is significantly disturbed with deviations of 1–9 pm from the optimal plane. The

Scheme 2. Synthesis of Complexes 2 (Top) and 3 (Bottom)

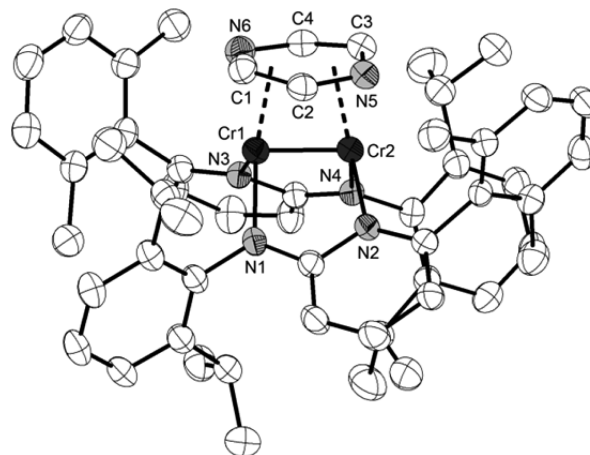
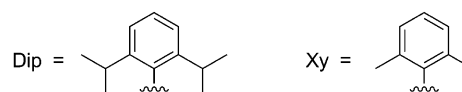
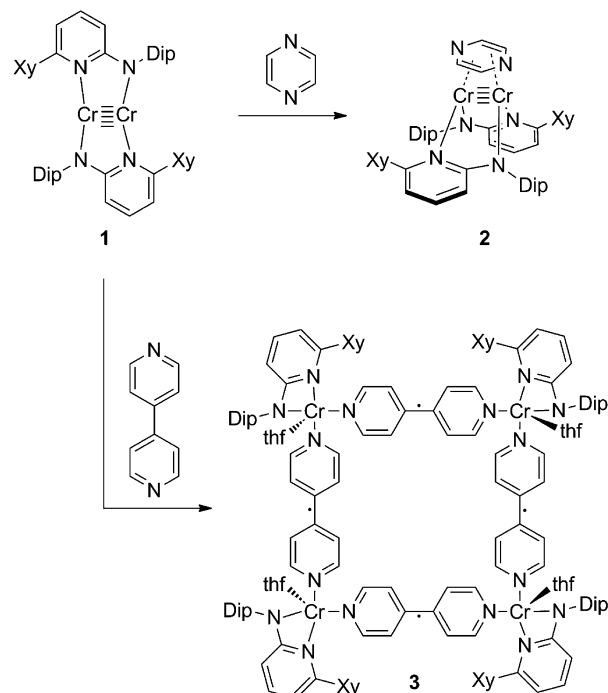


Figure 1. Molecular structure of **2** (hydrogen atoms have been omitted for clarity). Selected bond lengths (pm) and angles (deg): Cr1–Cr2 191.62(6), Cr1–N1 206.3(2), Cr1–N3 203.9(2), Cr2–N2 204.6(2), Cr2–N4 206.5(2), Cr1–C1 208.4(3), Cr1–C2 243.7(3), Cr1–N6 204.2(2), Cr1–C4 246.3(3), Cr2–C2 245.2(3), Cr2–N5 204.4(2), Cr2–C3 209.2(3), Cr2–C4 244.6(3); N1–Cr1–N3 102.14(8), N2–Cr2–N4 103.29(8).

corresponding C and N atoms of pyrazine were differentiated carefully, and the assignment can be justified by the similar size of the thermal ellipsoids in the ORTEP plot (Figure 1). C–C and C–N bond lengths fall in the range 138–141 pm, thus being similar to those of the only other crystallographically characterized metal complex with π -coordinated pyrazine, bis(tetramethylpyrazine)vanadium (137–141 pm).²⁰ The mean CNC angle of 112.4° is smaller than the average NCC

and CCN angles (125.3° and 120.8°). In combination with the Cr–Cr bond length this points toward a chromium(II) complex with a doubly reduced pyrazine ligand. As expected the ^1H and ^{13}C NMR spectra show a diamagnetic complex with a single set of signals for the symmetry-equivalent Ap ligands and highly shielded pyrazine signals ($\delta_{\text{H}} = 3.22$ ppm, $\delta_{\text{C}} = 90.6$ ppm), confirming the interpretation as dianionic N-heterocycle.

When **1** is reacted with 4,4'-bipyridine in THF, the molecular square **3** is obtained as blue crystals (Scheme 2, bottom). Cleaving of the metal–metal quintuple bond in contrast to the reduction of the bond order and the maintaining of the multiple bond has been previously observed for an aryl ligand stabilized dichromium complex if treated with N_2O and adamantanyl azide.^{11a} Further quintuple bond cleavage reactions have been reported by Theopold and co-workers^{3h} as well as by Tsai and co-workers.^{11b} The tetranuclear complex **3** contains chromium atoms with square-pyramidal coordination (the sums of angles within the CrN_4 planes lie between 359.7° and 360.2°) and THF ligands in the apical positions (Figure 2). The Cr–N bond lengths toward Ap ligands fall in

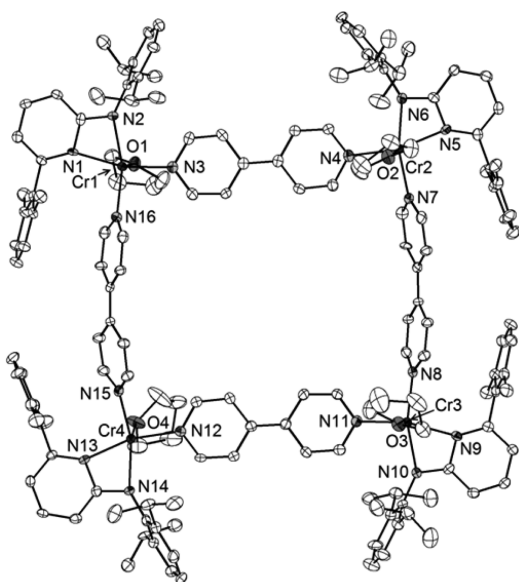


Figure 2. Molecular structure of **3** (hydrogen atoms, disordered positions, and crystal solvent have been omitted for clarity). Selected bond lengths (pm) and angles (deg): Cr1–N1 211.4(3), Cr1–N2 210.4(3), Cr1–N3 207.3(4), Cr1–N16 208.4(3), Cr2–N5 213.6(3), Cr2–N6 208.0(4), Cr2–N4 207.6(4), Cr2–N7 207.7(3), Cr3–N9 210.9(3), Cr3–N10 209.8(4), Cr3–N8 206.8(4), Cr3–N11 206.8(4), Cr4–N13 211.4(4), Cr4–N14 212.1(3), Cr4–N12 207.1(4), Cr4–N15 207.6(4); N3–Cr1–N16 95.21(14), N4–Cr2–N7 92.72(14), N8–Cr3–N11 94.92(14), N12–Cr4–N15 93.04(14).

the range 208–214 pm and are thus significantly longer than in **2**, which can presumably be rationalized by the increased coordination number. The Cr–N bond lengths toward 4,4'-bipyridine amount to 207–208 pm, rendering them virtually identical and short in comparison with values obtained for the nonreduced 4,4'-bipyridine ligand in **4** (231–237 pm, see below). The reduced nature of the N-heterocycles in **3** becomes apparent by looking at their central C–C bond lengths, which have a mean value of 142.2 pm and are thus significantly shorter than in free 4,4'-bipy (148.42(19) and 148.95(18) pm, respectively) while being longer than those in doubly reduced bis(trimethylsilyl)dihydro-4,4'-bipyridine

(138.1(3) pm).^{18b} Similar central C–C distances were in fact found in Ti-based supramolecular compounds (142–144 pm^{18b}), pointing toward an analogous electronic situation, i.e., the combination of a singly reduced 4,4'-bipy radical anion and chromium(II). According to this scenario, the torsion between the pyridyl rings ($2\text{--}15^\circ$) lies in the same range as in the titanium-based complexes.^{18b} Attempts to confirm the existence of **3** in solution (NMR, MS) failed. NMR data could not be obtained due to the paramagnetism observed for **3**. MS (ESI) signals were attempted to be obtained at various instruments but were unsuccessful.

Magnetic susceptibility measurements show that the observed $\chi_{\text{M}}T$ value of $13.3\text{ cm}^3\text{ K mol}^{-1}$ at room temperature increases nearly linearly down to 70 K (Figure 3). Below this

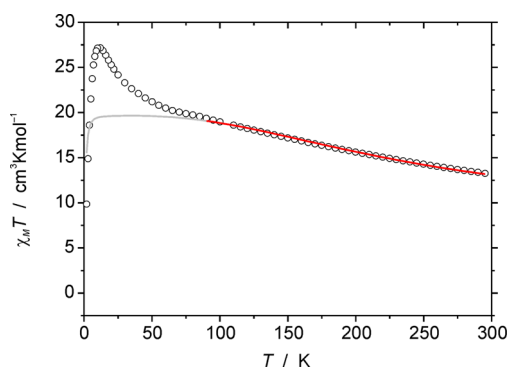


Figure 3. $\chi_{\text{M}}T$ vs T plot of **3** obtained from a SQUID measurement at 5000 Oe. The solid red line represents the calculated curve fit in the range 295–90 K; the gray line represents the theoretical curve progression for the used exchange model (see below).

temperature the $\chi_{\text{M}}T$ curve increases more rapidly, reaching a maximum of $27.2\text{ cm}^3\text{ K mol}^{-1}$ at 12 K. At even lower temperatures $\chi_{\text{M}}T$ drops, which may be due to the effects of zero-field splitting and/or intermolecular antiferromagnetic interactions. According to the molecular structure of **3**, only one unique exchange interaction pathway exists between neighboring chromium(II) ions ($S = 2$) and radical ligands ($S = 1/2$) (Figure 4, left). If we assume that this exchange

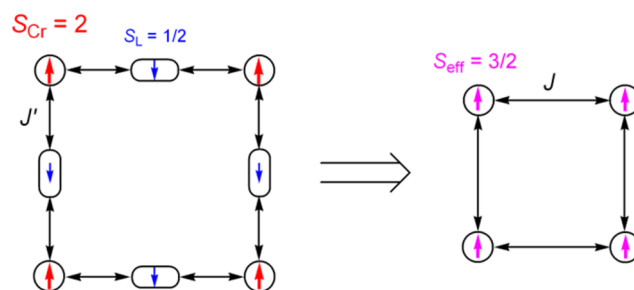


Figure 4. Coupling scheme for **3** in full (left) and simplified (right) form.

interaction is ferromagnetic, a large spin ground state of $S_{\text{T}} = 4 \cdot 2 + 4 \cdot 1/2 = 10$ should result. The expected $\chi_{\text{M}}T$ value is $55.0\text{ cm}^3\text{ K mol}^{-1}$ at low temperatures, which is much higher than the experimentally observed value. The alternative case, i.e., antiferromagnetic interaction between chromium(II) ions and radical ligands, leads to $S_{\text{T}} = 4 \cdot 2 - 4 \cdot 1/2 = 6$ and a theoretical $\chi_{\text{M}}T$ value of $21.0\text{ cm}^3\text{ K mol}^{-1}$, which is closer to the experimental value. Since antiferromagnetic coupling between

nonequivalent spin carriers ($S = 2$ and $S = 1/2$ in this case) leads to noncompensated magnetic moments that are ferromagnetically coupled (i.e., ferrimagnetic alignment), and since an exact model with eight spin carriers exceeds our present computational possibilities, for further preliminary analysis we assume an effective spin state ($S_{\text{eff}} = 3/2$) as the result of antiferromagnetic coupling between a high-spin chromium(II) ion ($S_{\text{Cr}} = 2$) and a ligand radical ($S_{\text{L}} = 1/2$). Four such effective spins are then coupled ferromagnetically (Figure 4, right). The appropriate Heisenberg–Dirac–van Vleck (HDvV) spin Hamiltonian includes a single isotropic exchange coupling constant and Zeeman splitting:

$$\hat{H} = -2J(\hat{S}_1\hat{S}_2 + \hat{S}_2\hat{S}_3 + \hat{S}_3\hat{S}_4 + \hat{S}_1\hat{S}_4) + g\mu_{\text{B}}\vec{B} \sum_{i=1}^4 \vec{S}_i$$

Best fit parameters are $g = 1.94$, $J = +30.5 \text{ cm}^{-1}$, and $\text{TIP} = 13 \times 10^{-6} \text{ cm}^3 \text{ mol}^{-1}$ (TIP = temperature-independent paramagnetism), but it should be noted that the increase of the $\chi_{\text{M}}T$ value curve below 70 K is not well-reproduced by this simplified model. The coupling scheme applied here is a severely simplified one, and the analysis and discussion of the magnetic data has to be regarded as preliminary. However, the size of the system with eight spin centers, and the lack of information about structural changes that may occur upon removal of (at least part of) the THF solvent molecules in the crystal lattice when preparing the dried samples for SQUID measurements, precludes a more detailed analysis at this stage.

Upon slow diffusion of a pyrazine-containing THF solution into a solution of **3**, red crystals of the porous coordination polymer **4** were obtained (Figure 5). The coordination sphere around chromium is again square-pyramidal (the sums of angles within the CrN_4 planes lie between 358° and 359°), but this time the Ap ligand and one pyrazine and 4,4'-bipyridine each form the basis while the second bipyridine ligand occupies the apical position. The Cr–N bond lengths toward the Ap ligands (209–210 pm) are comparable to those within **3**, but the ones toward the bridging ligands fall into two separate groups. While the Cr–N bonds within the molecular rectangle as shown in Figure 5 are short (202–206 pm), the Cr–N bonds of the remaining apical 4,4'-bipyridine are substantially longer (231 and 237 pm). In agreement with these findings the central C–C bond lengths amount to about 143 pm for the bipyridine ligands within the molecular rectangle, which is consistent with a formulation as radical anions. The 4,4'-bipyridine bridging the rectangles via the apical coordination sites, however, shows central C–C bond lengths of 148 pm which point toward a nonreduced heterocycle. This leads to the conclusion that the description of **4** as a molecular rectangle with additional bridging ligands is indeed not only an arbitrary way of visualizing this polymeric structure, but represents the electronic situation. Within the rectangle, all bridging ligands (both pyrazine and 4,4'-bipyridine) are radical anions; they connect chromium(II) centers as in **3**. The remaining neutral, nonreduced 4,4'-bipyridine connects these tetranuclear moieties, forming a coordination polymer. This assumption is also supported by the magnetic properties of **4**.

The $\chi_{\text{M}}T$ curve of **4** increases from $13.3 \text{ cm}^3 \text{ K mol}^{-1}$ at 295 K to $18.7 \text{ cm}^3 \text{ K mol}^{-1}$ at 25 K, and then drops at even lower temperatures, which may be due to the effects of zero-field splitting and/or intermolecular antiferromagnetic interactions (Figure 6). Magnetic properties of **4** can be rationalized in a similar way as described for **3**: four chromium(II) ions and four

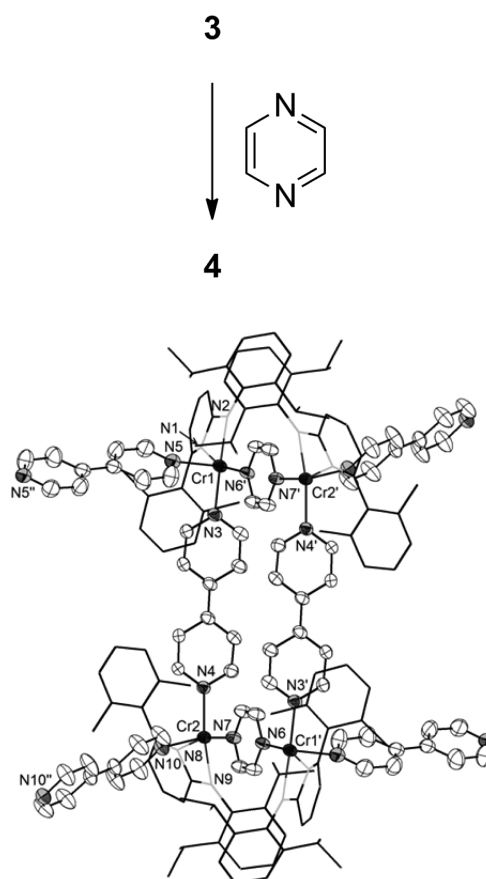


Figure 5. Synthesis and structure of **4**. Only metal atoms and bridging ligands are shown (hydrogen atoms and crystal solvent have been omitted for clarity). Selected bond lengths (pm) and angles (deg): Cr1–N_{pyridine(Ap)} 210.4(4), Cr1–N_{amido(Ap)} 209.3(4), Cr1–N1 205.3(4), Cr1–N3 236.5(4), Cr1–N4 202.0(4), Cr2–N_{pyridine(Ap)} 210.3(4), Cr2–N_{amido(Ap)} 209.8(4), Cr2–N2 206.2(4), Cr2–N6 230.9(4), Cr2–N5 201.8(4); N2–Cr1–N4 93.30(14), N1–Cr1–N3 95.18(15), N3–Cr1–N4 90.70(16), N2–Cr2–N5 93.28(14), N2–Cr2–N6 101.80(15), N5–Cr2–N6 87.62(14).

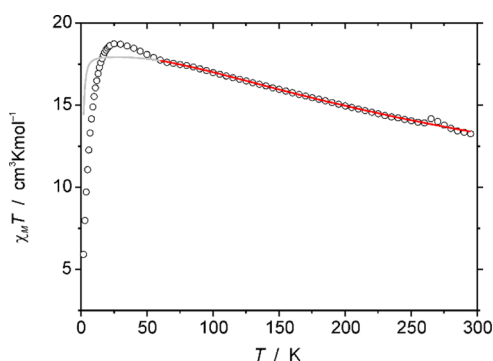


Figure 6. $\chi_{\text{M}}T$ vs T plot of **4** obtained from a SQUID measurement at 5000 Oe. The solid red line represents the calculated curve fit in the range 295–60 K; the gray line represents the theoretical curve progression for the used exchange coupling model (see Supporting Information Figure S1).

radical ligands are antiferromagnetically coupled, which leads to ferromagnetic alignment of effective spins $S_{\text{eff}} = 3/2$ and results in an $S_{\text{T}} = 6$ ground state for the Cr_4 rectangular unit (the magnetic coupling through long nonreduced 4,4'-bipyridine linkers connecting such Cr_4 units was neglected). However,

according to the molecular structure of **4**, two different exchange interaction pathways, i.e., via the pyrazine radical and via the 4,4'-bipyridine radical (Supporting Information Figure S1), should be assumed.

The porous coordination polymer **4** is very sensitive toward hydrolysis and oxidation. Although it can be dried without decomposition as shown by powder diffraction of a dried sample (Figure 7), adsorption of N₂ into the porous structure

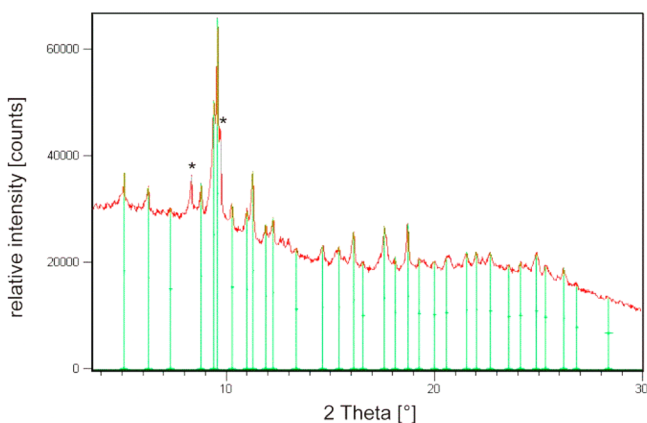


Figure 7. Powder XRD analysis of **4**. Red and green lines show the observed and simulated peaks, respectively. * represents the presence of **3** as an impurity.

could not be detected. It should be noted, however, that N₂ was also not adsorbed by the nanotubular material obtained by polymerization of Pt-based molecular squares.¹⁹ Thermogravimetric measurements showed that **4** is stable up to 150 °C under inert conditions.

CONCLUSIONS

In summary it was shown that metal–metal bond cleavage can be used as a new tool for the synthesis of molecular squares. The reaction of a quintuply bonded chromium(I) dimer with the classical linker 4,4'-bipyridine yielded a chromium(II)-based molecular square with reduced bridging N-heterocycles. Selective polymerization of this compound gave rise to a porous coordination polymer.

EXPERIMENTAL SECTION

Synthesis of Compounds. *Synthesis of 2.* A solution of pyrazine (0.019 g, 0.24 mmol) in hexane (5 mL) was layered over a solution of **1** (0.2 g, 0.24 mmol) in THF (10 mL) and was allowed to stand at room temperature for a couple of days causing the solution to turn brown-green. The volume of solvent was then reduced to one-third to afford crystals of **2** at room temperature. Crystals were separated by filtration and washed with hexane (ca. 5 mL). The filtrate was used to

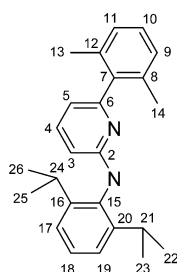


Figure 8. Labeling of the NMR signals.

afford further crystals of the product. Yield: 0.156 g (67%). C₅₄H₆₂Cr₂N₆·C₄H₈O (971.21): calcd C 71.73, H 7.26, N 8.65%; found C 71.40, H 7.08, N 8.72%. ¹H NMR (400 MHz, C₆D₆): δ = 1.02 (br d, 12H, H^{22,23,25,26}), 1.10 (br d, 12H, H^{22,23,25,26}), 1.42 (s, 12H, H^{13,14}), 1.53 (br s, 4H, cocrystallized THF), 3.22 (br m, 6H, H^{21,24} and pyrazine), 3.75 (sept, 2H, H^{21,24}), 5.86 (d, 2H, J = 5.6 Hz, H³), 6.16–6.26 (m, 4H, H^{5,10,18}), 6.54 (d, 2H, J = 5.2 Hz, H^{9,11}), 6.67–6.71 (m, 4H, H^{10,18,4}), 6.82 (br, 2H, H^{9,11}), 7.22 (m, 4H, H^{9,11,17,19}) ppm. ¹³C NMR (100 MHz, C₆D₆): δ = 18.4 (C^{13,14}), 20.2 (C^{13,14}), 24.1 (C^{22,23,25,26}), 24.4 (C^{22,23,25,26}), 25.8 (cocrystallized THF), 25.8 (C^{22,23,25,26}), 26.3 (C^{22,23,25,26}), 26.9 (C^{21,24}), 28.1 (C^{21,24}), 67.8 (cocrystallized THF), 90.6 (br, pyrazine), 110.2 (C³), 111.2 (C⁵), 123.8 (C¹⁰), 124.8 (C¹⁸), 125.4 (C^{17,19}), 126.4 (C^{17,19}), 127.1 (C^{9,11}), 135.3 (C^{8,12}), 135.6 (C^{8,12}), 138.2 (C⁴), 139.1 (C⁷), 144.0 (C^{16,20}), 146.0 (C^{16,20}), 147.0 (C¹⁵), 160.2 (C⁶), 168.2 (C²) ppm.

Synthesis of 3. A solution of 4,4'-bipyridine (0.076 g, 0.48 mmol) in THF (5 mL) was layered slowly over a solution of **1** (0.2 g, 0.24 mmol) in THF (10 mL), causing the solution to gradually turn blue. The mixture was kept at room temperature for a couple of days to afford blue crystals suitable for X-ray analysis. Yield: 0.15 g (49%). C₁₅₆H₁₈₀Cr₄N₁₆O₄ (2551.19): calcd C 73.44, H 7.11, N 8.78%; found C 72.96, H 6.80, N 9.25%. For details on magnetic measurements, see below. IR (Fomblin YR-1800, 26 °C, cm⁻¹): 3053 (v), 2954 (w), 2863 (w), 1591 (s), 1547 (w), 1439 (s), 1400 (w), 1357 (w), 1314 (w), 1246 (s), 1192 (s), 1152 (m), 1064 (w), 1040 (m), 1010 (m), 998 (w), 958 (s), 899 (s), 855 (w), 802 (w), 767 (s), 740 (m), 684 (m), 621 (s), 570 (v), 557 (v), 504 (m), 460 (v), 432 (w).

Synthesis of 4. A solution of pyrazine (0.011 g, 0.136 mmol) in THF (2 mL) was layered slowly over a solution of **3** (0.1 g, 0.0392 mmol) in THF (10 mL), causing the solution to gradually turn brown-red. The solution was kept at room temperature for a couple of days to afford red crystals suitable for X-ray analysis. Yield: 0.064 g (68%). C₁₄₈H₁₅₆Cr₄N₂₀ (2422.91): calcd C 73.36, H 6.49, N 11.56%; found C 73.67, H 6.51, N 11.66%. For details on magnetic measurements, see the Supporting Information. IR (Fomblin YR-1800, 26 °C, cm⁻¹): 2955 (w), 2862 (w), 1595 (s), 1548 (w), 1455 (s), 1307 (v), 1231 (s), 1193 (m), 1151 (m), 1040 (s), 958 (s), 777 (m), 732 (m), 686 (w), 563 (v).

Magnetic Measurements. Temperature-dependent magnetic susceptibility data were measured using a Quantum-Design MPMS-XL-5 SQUID magnetometer, operating in the range from 295 to 2 K at a magnetic field of 5000 Oe. The powdered sample was contained in a gel bucket and fixed in a nonmagnetic sample holder. Each raw data file for the measured magnetic moment was corrected for the diamagnetic contribution of the sample holder and the gel bucket. Molar susceptibility data were corrected for the diamagnetic contribution. Full-matrix diagonalization of exchange coupling and Zeeman splitting was performed with the *julX* program.²¹

ASSOCIATED CONTENT

Supporting Information

General experimental considerations, crystallographic details (including CIF data), magnetic susceptibility data of **4**, and TGA of **4**. This material is available free of charge via the Internet at <http://pubs.acs.org>.

AUTHOR INFORMATION

Corresponding Author

*E-mail: kempe@uni-bayreuth.de. Fax: (+49)921-55-2157.

Present Address

[†]Fachbereich Chemie, Technische Universität Kaiserslautern, Erwin-Schrödinger-Straße 54, 67663 Kaiserslautern, Germany.

Notes

The authors declare no competing financial interest.

ACKNOWLEDGMENTS

This work was supported by the Deutsche Forschungsgemeinschaft (DFG KE 756/20-2). E.S.T. thanks the Deutsche Akademische Austauschdienst (DAAD) for a Ph.D. stipend. We thank Dr. Hussein Kalo for IR measurements.

REFERENCES

- (1) (a) Wagner, F. R.; Noor, A.; Kempe, R. *Nat. Chem.* **2009**, *1*, 529–536. (b) Cotton, F. A.; Murillo, L. A.; Walton, R. A. *Multiple Bonds Between Metal Atoms*, 3rd ed.; Springer: Berlin, 2005. Nair, A. K.; Satyachand Harisomayajula, N. V.; Tsai, Y. C. *Dalton Trans.* **2014**, *43*, 5618–5638. Satyachand Harisomayajula, N. V.; Nair, A. K.; Tsai, Y. C. *Chem. Commun.* **2014**, 3391–3412.
- (2) Nguyen, T.; Sutton, A. D.; Brynda, M.; Fettingner, J. C.; Long, G. J.; Power, P. P. *Science* **2005**, *310*, 844–847.
- (3) (a) Kreisel, K. A.; Yap, G. P. A.; Dmitrenko, O.; Landis, C. R.; Theopold, K. H. *J. Am. Chem. Soc.* **2007**, *129*, 14162–14163. (b) Wolf, R.; Ni, C.; Nguyen, T.; Brynda, M.; Long, G. J.; Sutton, A. D.; Fischer, R. C.; Fettingner, J. C.; Hellman, M.; Pu, L.; Power, P. P. *Inorg. Chem.* **2007**, *46*, 11277–11290. (c) Noor, A.; Wagner, F. R.; Kempe, R. *Angew. Chem.* **2008**, *120*, 7356–7359; *Angew. Chem., Int. Ed.* **2008**, *47*, 7246–7249. (d) Tsai, Y.-C.; Hsu, C.-W.; Yu, J.-S. K.; Lee, G.-H.; Wang, Y.; Kuo, T.-S. *Angew. Chem.* **2008**, *120*, 7360–7363; *Angew. Chem., Int. Ed.* **2008**, *47*, 7250–7253. (e) Hsu, C.-W.; Yu, J.-S. K.; Yen, C.-H.; Lee, G.-H.; Wang, Y.; Tsai, Y.-C. *Angew. Chem.* **2008**, *120*, 10081–10084; *Angew. Chem., Int. Ed.* **2008**, *47*, 9933–9936. (f) Noor, A.; Glatz, G.; Müller, R.; Kaupp, M.; Demeshko, S.; Kempe, R. *Z. Anorg. Allg. Chem.* **2009**, *635*, 1149–1152. (g) Noor, A.; Bauer, T.; Todorova, T. K.; Weber, B.; Gagliardi, L.; Kempe, R. *Chem.—Eur. J.* **2013**, *19*, 9825–9832. (h) Shen, J.; Yap, G. A.; Theopold, K. H. *Chem. Commun.* **2014**, *50*, 2579–2581. (i) Shen, J.; Yap, G. A.; Theopold, K. H. *J. Am. Chem. Soc.* **2014**, *136* (9), 3382–3384.
- (4) (a) Tsai, Y.-C.; Chen, H.-Z.; Chang, C.-C.; Yu, J.-S. K.; Lee, G.-H.; Wang, Y.; Kuo, T.-S. *J. Am. Chem. Soc.* **2009**, *131*, 12534–12535. (b) Liu, S.-C.; Ke, W.-L.; Yu, J.-S. K.; Kuo, T.-S.; Tsai, Y.-C. *Angew. Chem.* **2012**, *124*, 6500–6503; *Angew. Chem., Int. Ed.* **2012**, *51*, 6394–6397. (c) Chen, H.-Z.; Liu, S.-C.; Yen, C.-H.; Yu, J.-S. K.; Shieh, Y.-J.; Kuo, T.-S.; Tsai, Y.-C. *Angew. Chem.* **2012**, *124*, 10488–10492; *Angew. Chem., Int. Ed.* **2012**, *51*, 10342–10346. (d) Chen, H.-G.; Hsueh, H.-W.; Kuo, T.-S.; Tsai, Y.-C. *Angew. Chem.* **2013**, *125*, 10446–10450; *Angew. Chem., Int. Ed.* **2013**, *52*, 10256–10260. (e) Carrasco, M.; Curado, N.; Maya, C.; Peloso, R.; Rodríguez, A.; Ruiz, E.; Alvarez, S.; Carmona, E. *Angew. Chem.* **2013**, *125*, 3309–3313; *Angew. Chem., Int. Ed.* **2013**, *52*, 3227–3231. (f) Carrasco, M.; Curado, N.; Alvarez, S.; Maya, C.; Peloso, R.; Poveda, M. L.; Rodríguez, A.; Ruiz, E.; Alvarez, S.; Carmona, E. *Chem.—Eur. J.* **2014**, *20*, 6092–6102.
- (5) Clouston, L. J.; Siedschlag, R. B.; Rudd, P. A.; Planas, N.; Hu, S.; Miller, A. D.; Gagliardi, L.; Lu, C. C. *J. Am. Chem. Soc.* **2013**, *135*, 13142–13148.
- (6) (a) Noor, A.; Kempe, R. *Chem. Rec.* **2010**, *10*, 413–416. (b) Harisomayajula, N. V. S.; Nair, A. K.; Tsai, Y.-C. *Chem. Commun.* **2014**, *50*, 3391–3412. (c) Nair, A. K.; Harisomayajula, N. V. S.; Tsai, Y.-C. *Dalton Trans.* **2014**, *43*, 5618–5638. (d) Noor, A.; Kempe, R. *Inorg. Chim. Acta* **2014**, doi: <http://dx.doi.org/10.1016/j.ica.2014.08.030>. (e) Nair, A. K.; Harisomayajula, N. V. S.; Tsai, Y.-C. *Inorg. Chim. Acta* **2014**, doi: <http://dx.doi.org/10.1016/j.ica.2014.09.020>.
- (7) (a) Landis, C. R.; Weinhold, F. *J. Am. Chem. Soc.* **2006**, *128*, 7335–7345. (b) Merino, G.; Donald, K. J.; D'Acchioli, J. S.; Hoffmann, R. *J. Am. Chem. Soc.* **2007**, *129*, 15295–15302. (c) LaMacchia, G.; Li Manni, G.; Todorova, T. K.; Brynda, M.; Aquilante, F.; Roos, B. O.; Gagliardi, L. *Inorg. Chem.* **2010**, *49*, 5216–5222. (d) Wu, L.-C.; Hsu, C.-W.; Chuang, Y.-C.; Lee, G.-H.; Tsai, Y.-C.; Wang, Y. *J. Phys. Chem. A* **2011**, *115*, 12602–12615.
- (8) (a) Noor, A.; Sobgwi Tamne, E.; Qayyum, S.; Bauer, T.; Kempe, R. *Chem.—Eur. J.* **2011**, *17*, 6900–6903. (b) Shen, J.; Yap, G. P. A.; Werner, J.-P.; Theopold, K. H. *Chem. Commun.* **2011**, *47*, 12191–12193.
- (9) Noor, A.; Glatz, G.; Müller, R.; Kaupp, M.; Demeshko, S.; Kempe, R. *Nat. Chem.* **2009**, *1*, 322–325.
- (10) (a) Schwarzmaier, C.; Noor, A.; Glatz, G.; Zabel, M.; Timoshkin, A. Y.; Cossairt, B. M.; Cummins, C. C.; Kempe, R.; Scheer, M. *Angew. Chem.* **2011**, *123*, 7421–7424; *Angew. Chem., Int. Ed.* **2011**, *50*, 7283–7286. (b) Sobgwi Tamne, E.; Noor, A.; Qayyum, S.; Bauer, T.; Kempe, R. *Inorg. Chem.* **2013**, *52*, 329–336. (c) Noor, A.; Qayyum, S.; Bauer, T.; Schwarz, S.; Weber, B.; Kempe, R. *Chem. Commun.* **2014**, *50*, 13127–13130.
- (11) (a) Ni, C.; Ellis, B. D.; Long, G. J.; Power, P. P. *Chem. Commun.* **2009**, 2332–2334. (b) Wu, P.-F.; Liu, S.-C.; Shieh, Y.-J.; Kuo, T.-S.; Lee, G.-H.; Wang, Y.; Tsai, Y.-C. *Chem. Commun.* **2013**, *49*, 4391–4393.
- (12) Selected reviews: (a) Fujita, M.; Ogura, K. *Coord. Chem. Rev.* **1996**, *148*, 249–264. (b) Olenyuk, B.; Fechtenkötter, A.; Stang, P. J. *J. Chem. Soc., Dalton Trans.* **1998**, 1707–1728. (c) Fujita, M. *Chem. Soc. Rev.* **1998**, *27*, 417–425. (d) Slone, R. V.; Benkstein, K. D.; Bélanger, S.; Hupp, J. T.; Guzei, I. A.; Rheingold, A. L. *Coord. Chem. Rev.* **1998**, *171*, 221–243. (e) Leiniger, S.; Olenyuk, B.; Stang, P. J. *Chem. Rev.* **2000**, *100*, 853–908. (f) Swiegers, G. F.; Malefets, T. J. *Coord. Chem. Rev.* **2002**, *225*, 91–121. (g) Lee, S. J.; Hupp, J. T. *Coord. Chem. Rev.* **2006**, *250*, 1710–1723. (h) Lee, S. J.; Lin, W. *Acc. Chem. Res.* **2008**, *41*, 521–537. (i) Zangrando, E.; Casanova, M.; Alessio, E. *Chem. Rev.* **2008**, *108*, 4979–5013. (j) Northrop, B. H.; Zheng, Y.-R.; Chi, K.-W.; Stang, P. J. *Acc. Chem. Res.* **2009**, *42*, 1554–1563. (k) Safont-Sempere, M. M.; Fernández, G.; Würthner, F. *Chem. Rev.* **2011**, *111*, 5784–5814. (l) Chakrabarty, R.; Mukherjee, P. S.; Stang, P. J. *Chem. Rev.* **2011**, *111*, 6810–6918 and references cited therein. (m) Newton, G. N.; Nihei, M.; Oshio, H. *Eur. J. Inorg. Chem.* **2011**, 3031–3042. (n) Chifotides, H. T.; Dunbar, K. R. *Acc. Chem. Res.* **2013**, *46*, 894–906.
- (13) Fujita, M.; Yazaki, J.; Ogura, K. *J. Am. Chem. Soc.* **1990**, *112*, 5645–5647.
- (14) Stang, P. J.; Cao, D. H.; Saito, S.; Arif, A. M. *J. Am. Chem. Soc.* **1995**, *117*, 6273–628.
- (15) Kraft, S.; Beckhaus, R.; Haase, D.; Saak, W. *Angew. Chem.* **2004**, *116*, 1609–1614; *Angew. Chem., Int. Ed.* **2004**, *43*, 1583–1587S.
- (16) Conrady, F. M.; Fröhlich, R.; Schulte to Brinke, C.; Pape, T.; Hahn, F. E. *J. Am. Chem. Soc.* **2011**, *133*, 11496–11499.
- (17) (a) Hahn, F. E.; Radloff, C.; Pape, T.; Hepp, A. *Organometallics* **2008**, *27*, 6408–6410. (b) Radloff, C.; Hahn, F. E.; Pape, T.; Fröhlich, R. *Dalton Trans.* **2009**, 7215–7222. (c) Radloff, C.; Weigand, J. J.; Hahn, F. E. *Dalton Trans.* **2009**, 9392–9394. (d) Schmidtendorf, M.; Pape, T.; Hahn, F. E. *Angew. Chem.* **2012**, *124*, 2238–2241; *Angew. Chem., Int. Ed.* **2012**, *51*, 2195–2198. (e) Schmidtendorf, M.; Pape, T.; Hahn, F. E. *Dalton Trans.* **2013**, *42*, 16128–16141.
- (18) (a) Kraft, S.; Hanuschek, E.; Beckhaus, R.; Haase, D.; Saak, W. *Chem.—Eur. J.* **2005**, *11*, 969–978. (b) Theilmann, O.; Saak, W.; Haase, D.; Beckhaus, R. *Organometallics* **2009**, *28*, 2799–2807.
- (19) Otsubo, K.; Wakabayashi, Y.; Ohara, J.; Yamamoto, S.; Matsuzaki, H.; Okamoto, H.; Nitta, K.; Uruga, T.; Kitagawa, H. *Nat. Mater.* **2011**, *10*, 291–295.
- (20) (a) McGhee, W. D.; Sella, A.; O'Hare, D.; Cloke, F. G. N.; Mehnert, C.; Green, M. L. H. *J. Organomet. Chem.* **1993**, *459*, 125–130. (b) Nowotny, M.; Elschenbroich, C.; Behrendt, A.; Massa, W.; Wocadlo, S. *Z. Naturforsch., B: Chem. Sci.* **1993**, *48*, 1581–1588.
- (21) Bill, E. *JulX: A Program for the Simulation and Analysis of Magnetic Susceptibility Data, V. 1.4*; Max Planck Institute for Chemical Energy Conversion: Mülheim/Ruhr, Germany, 2008.